Lateral load testing and 3D stress measurements in a pile foundation

Rabie Farrag [i], Volker Slowik[ii] and Anne Lemnitzer [iii]

i) Postdoctoral fellow, Department of Civil and Environmental Engineering, University of CA, Irvine, Irvine, USA

ii) Professor, Faculty of Civil Engineering, Leipzig University of Applied Sciences, Leipzig, Germany

iii) Associate Professor, Department of Civil and Environmental Engineering, University of CA, Irvine, Irvine, USA

ABSTRACT

Embedded sensors within infrastructure elements are powerful catalysts for new designs and construction methods, enabling advanced data collection and informed decision making. This paper presents the development, validation, and implementation of a prototype instrumentation tool utilized in large-scale lateral load tests of rock-socketed pile foundations, with the objective to measure shear stresses near the rock-soil boundary. The proposed instrumentation is novel in that it will be the first attempt to determine experimentally the 3D strain field through embedded sensors with immediate application to a broad array of pile foundation engineering problems. Data obtained from the prototype instrumentation is used to clarify whether shear force amplifications in piles crossing soils with strong stiffness contrasts are real, or an artifact of analytical, Winkler-based design methodologies. Three reinforced concrete pile specimens with a diameter of 0.46 m and a length of 4.9 m were subjected to reverse cyclic lateral loading up to complete structural failure. The sensors' development, design, and construction, as well as their performance in measuring shear stresses will be discussed by comparing experimental data with predictions from conventional software tools. Ultimately, this study aims to improve the design and construction of more practical, resilient, and economical infrastructure.

Keywords: lateral loading, stiffness contrast, rock sockets, shear demands, strain measurements

1 INTRODUCTION

Laterally loaded piles embedded in rock provide an attractive solution to transmit large forces and overturning moments into the ground. In many cases, pile extension into bedrock (i.e., rock-socketing) represents the only constructable solution to provide sufficient lateral restraint when ground conditions in upper bearing layers are insufficiently strong. Simultaneously, rock-socketed pile design has historically challenged design engineers as the pile structural response near the rock-soil interface is driven by the stiffness contrast between rock and surface soils. Particularly, predictions using Winkler-type analyses yield abrupt changes in the pile moment profile which translates into amplified shear forces at the interface of very stiff and very soft geomaterial layers. The validation of shear amplification predicted with the *p-y* method against instrumented load tests or validated numerical models is limited in existing literature. However, when shear demands govern the structural design of drilled piles, the correct evaluation of shear forces at soil-rock interfaces is vital. High shear demands require either high transverse reinforcement ratios or an increase in the pile diameter, both of which impact the overall constructability and cost of the foundation system. Numerical research has attempted to provide insight into the principal mechanism (e.g., Arduino et al., 2018), but no experimental data are available to date that can provide sufficient fundamental understanding to advance alternative design recommendations suitable for routine practice. The lack of experimental pile shear data is largely driven by our inability to directly measure internal shear stresses experimentally. Therefore, the pile shear and moments are obtained through differentiating the fourth-order differential Euler-

Bernoulli Beam equation, and relating geomaterial reactions to internal pile reactions. Thus, the shear demands are based on the assumptions of the Euler-Bernoulli theory which neglects shear deformations and assumes plane sections to remain plane. To address the lack of experimental shear measurements and to further investigate the amplified shear demands of piles in soils with strong stiffness contrasts, three large-scale, rock-socketed pile specimens were tested experimentally to complete structural failure. Two specimens were designed to fail near the rock-soil interface where the predicted shear spike occurs, and one specimen was designed with sufficient transverse reinforcement to sustain the amplification in shear forces suggested by analytical predictions. Two observations are of interest to this study: (a) the overall performance behavior and failure mechanism of all three pile specimens under identical geometric and loading conditions, and (b) the actual development of shear strains near the rock-socket boundary and the potential shear failure in this region.

To capture and quantify the shear demands experimentally, a prototype strain gauge-based measuring tool was developed, calibrated, and deployed to extract the internal three-dimensional strain tensor in cast-in-place concrete elements. To determine the strain tensor at any given point, three normal strains and six shearing strains must be known. Since there are only three independent shearing strains, the strain tensor is reduced to six independent strains. Therefore, a minimum of six normal strain components are needed to fully compute the strain tensor at any given location.

The measuring tool was made of a tetrahedral shaped 3D carrier (Fig. 1) which carries six strain gauges along its legs (i.e., yielding six normal strain components) and can be placed at the point of interest within the cast-in-place element. Its development and configuration was motivated by the previous work of Slowik et al., 1999. Prior, during, and after its placement within the rock-socketed pile specimens, the sensor was continuously evaluated and validated in small and model–scale testing of concrete elements (Farrag, 2021).

2 CARRIER DEVELOPMENT AND VALIDATION

The construction of the instrumentation tool underwent a lengthy development phase, which included a multitude of iterations on size, material, leg alignment, corner connections, overall construction sequence, and its ability to survive harsh loading conditions during pile construction (e.g., concrete placement). To comply with general principles of mechanics and the development of stress fields surrounding embedded objects, the dimensions of the tetrahedron carrier must be small compared to those of the host element and large compared to the aggregate size for concrete applications. Fig. 1 shows the final geometry and dimensions of the Tetrahedron skeleton. The upright position was selected to extend its configuration in future applications to truss-type instrumentation structures. The base legs have a length of 5.4 cm [2.125 in], and the height of the tetrahedron is 6.4 cm [2.5 in]. The diagonal struts measure 8.3 cm [3.3 in]. All legs were made of 0.6 cm [0.25 in] square acrylic rods. Acrylic was chosen for its low modulus of elasticity (approximately 10% of the concrete modulus) which reduces the variation in the strain field surrounding the tetrahedron. In addition, acrylic has a suitable range of compressive and tensile strength pertinent to the magnitude of strains expected for this application. It also provides excellent resistance to heat distortion, which is important for the attachment and soldering of strain gauges and wires to the tetrahedron legs, respectively.

The tetrahedra construction process had to be automated and optimized to minimize misalignments of tetrahedra legs, maintain identical global geometry and local corner connectivity, and ensure accurate attachment and central alignment of the strain gauges to each leg. Therefore, a 3D printed mold with grooves was developed to align and secure the carrier rods until the corners are connected through high-strength epoxy. A second mold was used to hold the specimen while each tetrahedron leg was furnished with one strain gauge. Given the carrier's material flexibility relative to that of the cast specimen, the embedded tetrahedron is expected to deform with the applied loading and could be used in a wide range of structures without significant impact on the mechanical behavior of its host.

The performance of the tetrahedral carriers was validated by embedding the sensors in a variety of host specimens, such as concrete cubes, concrete cylinders, and concrete beams, and subjecting them to sequentially applied, multidirectional loading (Farrag et al., 2022). The validation of the sensors embedded in a three-span concrete beam is described hereafter. The beam's structural configuration was selected in a manner so that known internal reactions such as shear and moment can be easily compared to experimental measurements obtained through external and internal instrumentation. The beam was 1.83 m [6 ft] long and had a square cross-section of 30.48 cm [1.0 ft]. Four tetrahedra named T1, T2, T3, and T4 were placed in the cross-sectional center and along the length of the beam as shown in Fig. 1. The beam was tested in a four-point setup (two load points, two support points). The loading configuration was designed to develop maximum shear and zero moment at the beam mid-span. Hooke's law can be utilized to obtain six components of stress from the measured strain within the linear elastic range when Young's modulus (E) and Poisson ratio are known. To determine these

parameters, concrete cylinders with dimensions of 15.2 cm [6 in] in diameter and 30.5 cm [12 in] in height were taken per ASTM C39 and mechanically tested per ASTM C469 to measure Young's modulus and Poisson's ratio at the day of beam testing. The beam concrete had an E-modulus and Poison ratio of 31 MPa [4.5 ksi] and 0.16, respectively. The beam was loaded within the linear elastic range following a non-destructive load test protocol. The load was applied in increments of 4.4 kN [1.0 kip] until a maximum load of 44 kN [10 kips] was reached. A similar pattern was followed for unloading. Shear strains measured through T1, T2, T3, and T4 were transformed into shear stresses at each respective location and compared to the statically calculated shear stresses as shown in Fig. 2. Measurements suggest that shear stresses recorded through the tetrahedra sensors are in good agreement with statically calculated shear stresses. A detailed description of this validation study including all stress transformations and assumptions regarding cross-sectional shear stress distribution can be found in Farrag 2021.

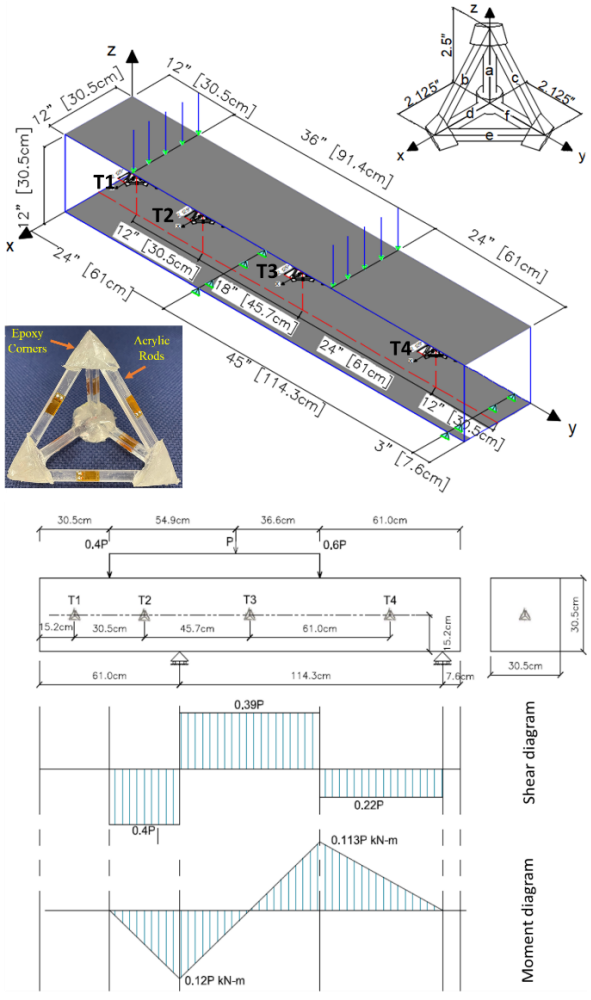

Fig. 1. The prototype tetrahedron sensor, the validation beam test setup, and shear and moment diagrams

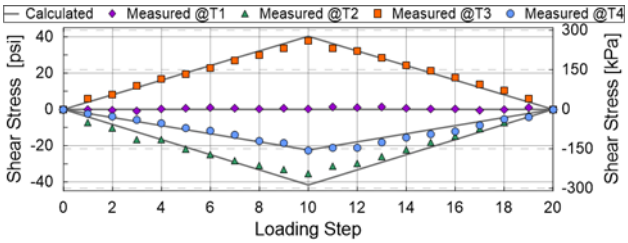

Fig. 2. Comparison of internal shear stresses obtained with tetrahedra instrumentation versus the statically calculated shear stresses.

3 EXPERIMENTAL PROGRAM

Following the promising results obtained during the validation testing, the tetrahedral sensors were deployed in the large-scale pile specimens described above. All experimental studies were executed in the "soil pit" at the Structural Engineering Testing Hall of the University of California, Irvine. The three test piles were embedded in a constructed sand-over-rock stratigraphy and subjected to reverse cyclic lateral loading. The rock formation was replicated experimentally through high-strength concrete blocks anchored to the bottom of the soil pit. The overlying sand layer consisted of poorly graded fill sand pluviated into the soil pit at a relative density of ~20-25%. Pile specimen design, construction history, testing procedures, and preliminary data analyses are presented in Lemnitzer et al., 2019, Farrag et al., 2020, and Farrag et al., 2021. The specimen design was based on analytical pre-test predictions using the commercially available software LPILE (Ensoft, 2018). The method of analysis (i.e., the Winkler-type analysis) is hereafter referred to generically as the "*p-y* method." The specimen design summary and the LPile input parameters are shown in Tables 1 and 2. According to predictions using Winkler-type analyses, significant shear forces were expected to develop just below the rock-socket surface, with the magnitude exceeding eight times the maximum applied lateral load at the pile head. Therefore, the tetrahedra sensors were placed within the rock-soil interface vicinity. Specifically, tetrahedra sensors were located at four different elevations starting 7.6 cm [3 inches] above the rock socket and spaced vertically downwards 15.2 cm [6 inches] apart. Fig. 3 (left) shows a generalized specimen configuration describing pile, rock-socket, and pile cap dimensions. Fig 3. (right) shows the tetrahedra layout of Specimen 1. The remainder of the instrumentation is omitted for

brevity since this paper focuses on the structural shear response only.

Table 1. Specimen Design Summary

	Specimen 1 (SP1)	Specimen 2 (SP2)	Specimen 3 (SP3)
Designed to satisfy	Amplified shear	Code minimum	Applied shear
Maximum shear demand V_u, kN [kips]	471 [106]	471 [106]	471 [106]
Selected transverse reinforcement, bar # @ pitch, mm [in]	Spiral #4 @ 114 [4.5]	Spiral #4 @ 152 [6]	Ties #3 @ 305[12]
Transverse reinf. volumetric ratio, ρ_s [%]	1.27%	0.95%	0.26%
Nominal shear strength V_n, kN [kips]	477 [107]	396 [89]	222 [50]
Predicted failure mode based on p-y analysis	Flexural failure	Shear failure	Shear failure

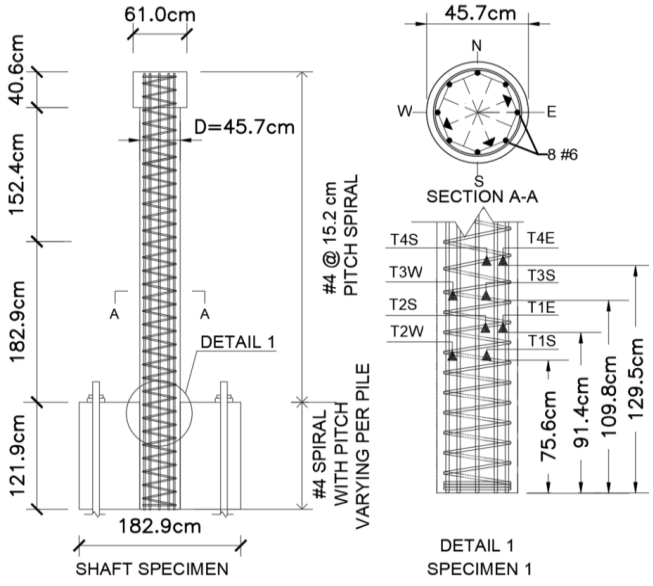

Fig. 3. Schematic specimen configuration and the tetrahedra layout of Specimen 1.

4 TEST RESULTS

The pile shear response was obtained through inverse analysis of the experimental tetrahedral strain data. The axial strain along the tetrahedral legs (ε_a, ε_b, ε_c, ε_d, ε_e, ε_f) can be rewritten as a function of the strain components in the tetrahedron's local rectangular system of coordinates (x ⊥ y ⊥ z) and the cosine of the directions cosine. axis X (E-W) ⊥ Y (N-S) ⊥ Z

Table 2. Model Input Parameters

Sand	p-y model	O'Neill and Murchison, 1983
	Effective unit weight	14.5kN/m3 [92 pcf]
	Friction Angle	35 deg
Pile	Model	Reinforced Concrete
	Compressive Strength	39.3 MPa [5.7 ksi]
Socket	p-y model	Reese et al., 1997
	Modulus	25.5 GPa [3695 ksi]
	Compressive Strength	48.3 MPa [7 ksi]
	Rock quality designation	100%
	strain factor	0.0005

The horizontal shear strain (γ_{XZ}) can then be translated into internal shear stress (τ_{XZ}) using Hooke's law. Therefore, the pile modulus and the Poisson's ratio were determined from cylinders tests of the pile concrete, performed on the day of pile testing and found to be 26.6 GPa [3856 ksi] and 0.2, respectively. The shear force (V) experienced by the pile cross-section can be estimated in terms of the shear stresses (τ_{XZ}), assuming that the shear stress distribution is symmetrically parabolic across the width (X-direction) of the pile cross-section and uniform shear stress across the thickness (Y-direction) of the cross-section following Equation 1.

$$V = \frac{3\pi R^4 . \tau_{XZ}}{4(R^2 - l^2)} \quad (1)$$

where R is the pile radius and l is the distance between the tetrahedron's geometric center to the peak shear stress. Fig. 4 shows an example of the recorded axial strains from the six individual strain gauges attached to the tetrahedron's legs (i.e., T3Sa through T3Sf), the calculated shear strain γ_{xz}, the shear stress τ_{xz}, and a comparison between the back-calculated shear force in the pile cross-section at location T3S and the applied shear force at the pile head. For Specimen 1, the tetrahedron T3S was located 12.7 cm [5 in] below the socket surface (maximum shear location) and away from the cross-section neutral axis by 6.4 cm [2.5 in].

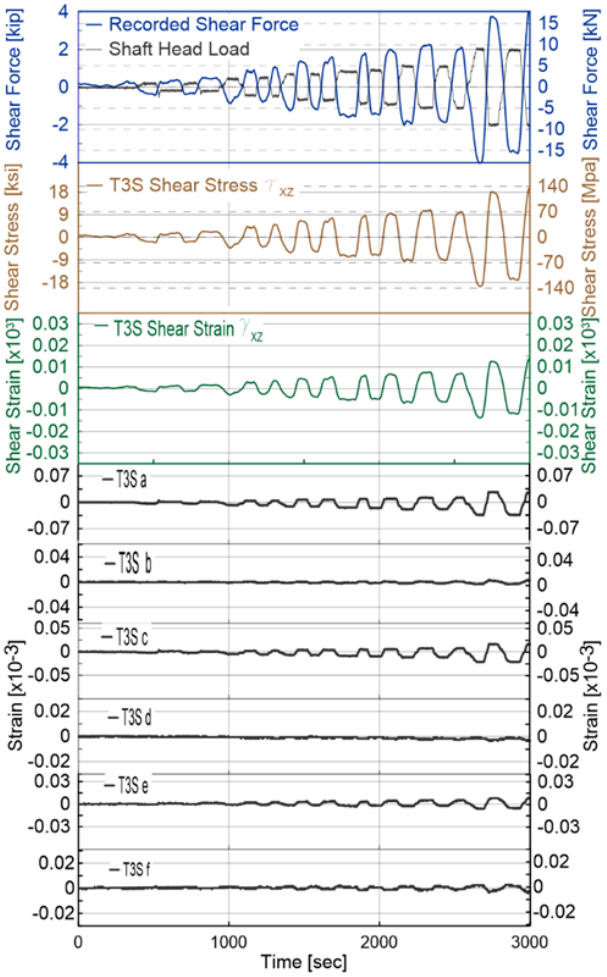

Fig. 4. Sample data histories for the recorded strain of sensor T3S in Specimen 1 at elevation 109.8 cm from the pile tip and the recorded amplified shear vs the applied load at the pile head.

Figure 5 illustrates the pile cross-section with stress contours, the placement of the tetrahedral sensors within the cross-section (see triangular symbols), and the stress data for push directions corresponding to this specific location (bottom). A quadratic fit across the pile diameter captures the measured pile stresses well and is in fundamental agreement with principles of cross-sectional shear stress distribution in mechanics. An integration of shear stresses within the area of the parabola yields the cross-sectional shear force for this specific elevation (i.e., T3S).

To quantitively study the observed shear amplification, the back-calculated shear force profile (using tetrahedral strains) was compared with the analytically predicted shear force profile as obtained with the *p-y* method (Fig. 5, right). For this comparison, pile responses due to an applied lateral load of 4.4kN [1.0 kip] at the pile head were selected. This particular choice was motivated by two criteria: (1) the selection enabled the shaft-rock system to remain elastic and the amplification ratio to be easily extractable (e.g., X:1); and (2) the 4.4kN [1.0 kip] load generates a strong amplification contrast which would not be achieved if the pile develops plastic deformations above the rock socket under higher lateral loading (since a plastic hinge will reduce the amount of shear transferred to the socket). Hence the chosen scenario replicates a "worst case," which is helpful to define the boundaries of the problem at hand. It could be further observed (Fig. 5, right) that the recorded amplification of 2.5 (the ratio between the applied lateral load and the maximum shear in the pile) is substantially less than the "p-y predicted" amplification of 13.5.

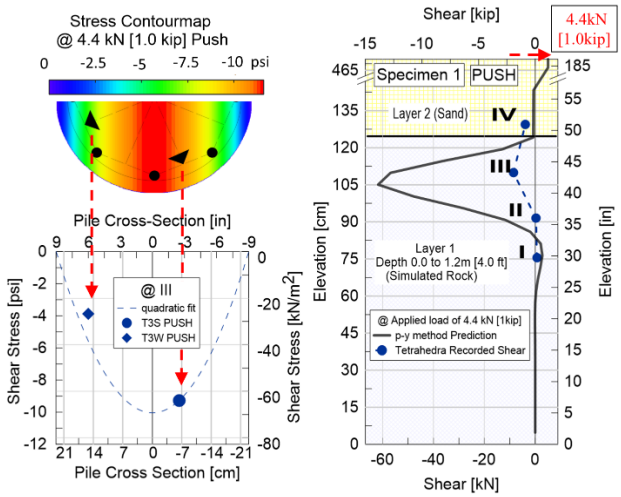

Fig. 5. The pile cross-sectional recorded shear stresses (left) and the pile shear profile comparisons of the recorded shear vs. the p-y predicted shear (right).

5 CONCLUSIONS

A three-dimensional prototype strain sensor was developed, calibrated, and deployed into a laterally loaded rock-socketed pile foundation with the objective to extract the internal three-dimensional strain tensor near the rock-soil interface. The sensors were first evaluated experimentally by embedding them into a concrete beam at a known internal shear stresses region. Measurements suggest that shear stresses recorded through the tetrahedra-shaped sensors are in good agreement with statically calculated shear stresses. Hereafter, the tetrahedral sensors were deployed in the large-scale pile specimens to capture the internal shear stresses at locations of interest. The embedded sensors allowed for a direct measurement of the internal shear strains and consecutive transformation into shear stresses which is a critical measurement to investigate the amplified shear demands of piles in soils with strong stiffness contrasts. The observed experimental shear amplification (the ratio between the applied load and

the maximum shear in the pile) was approximately 1/5 of the amplification predicted by a *p-y* type of analysis. The ratio of experimental amplification recorded near the rock-soil boundary and the applied lateral load at the pile head was approximately 2.5:1. Note that this ratio varies with the level of applied load at the pile head but remains much smaller than any analytically predicted magnification. This observation is critical to the design of rock-socketed foundation elements, as high transverse shear reinforcement in rock-socketed foundations has led to severe construction deficiencies due to the obstruction of concrete flow (i.e., poor concrete consolidation due to rebar congestion). The prototype tetrahedra represents the first successful attempt to determine experimentally the 3D strain field through embedded sensors in geo-structural elements and implies promising potential for further development and future application to a wide array of foundation components.

ACKNOWLEDGEMENTS

The experimental work was funded through the DFI Committee project fund, as well as through the first author's NSF funding (CMMI 1752303), along with generous industry support from our colleagues at DFI and ADSC. We would like to gratefully acknowledge the members of the DFI Drilled Shaft Committee, many of whom provided continuous feedback and guidance during the design and construction process of the piles [specifically Committee Chair Paul Axtell (Dan Brown and Associates), Peter Faust (Malcolm Drilling), Dr. Eric Loehr (Univ. of Missouri), and Dr. Armin Stuedlein (Oregon State University)]. We are furthermore extremely grateful for the material and equipment donations as well as the engineering support by: PJ Rebar (Nathan King), Atlas Geofoam (Chris Franks), Williams Form Engineering (Pete Speier and Jeff Ohlsen), Foundation Technologies, Inc. (Nick Milligan), and Gregg Drilling and Testing (Brian Savela and Kelly Cabal). Without the support of these colleagues, this research program would not have been possible in the scope described.

REFERENCES

1) Arduino, P., Chen, L., and McGann, C. (2018): Estimation of Shear Demands on Rock Socketed Drilled Shafts subjected to Lateral Loading, PEER Report, retrieved from https://peer.berkeley.edu/sites/default/files/2018_06arduino_final.pdf

2) ASTM C469 / C469M-21. (2021): Standard Test Method for Compressive Strength of Cylindrical Concrete Specimens, ASTM International, West Conshohocken, PA , www.astm.org

3) ASTM C39 / C39M-21. (2021): Standard Test Method for Compressive Strength of Cylindrical Concrete Specimens, ASTM International, West Conshohocken, PA, www.astm.org

4) Ensoft,Inc (2018) – LPILE User's Manual. A Program to Analyze Deep Foundations Under Lateral Loading. Austin, Texas.

5) Farrag, R., Cox, C., Turner,B., and Lemnitzer, A. (2020): Shear Demands of Rock-Socketed Shafts Subject to Cyclic Lateral Loading, Deep Foundations Journal, Volume 14, Issue 2, DFI Student Paper Award 2020, https://doi.org/10.37308/DFIJnl.202005

6) Farrag, R., Turner, B., Cox, C., and Lemnitzer, A. (2021): Experimental studies of rock socketed shafts with different transverse reinforcement ratios". International Foundations Congress and Equipment Expo (IFCEE), Dallas, Texas, May 10-14th, 2021.

7) Farrag, R. (2021): Experimental and Numerical Studies of Shear demands of rock-socketed drilled shafts, Dissertation, Civil and Environmental Engineering Department, University of California Irvine.

8) Farrag, R., Slowik, V., and Lemnitzer, A. (2022): Experimental evaluation of three-dimensional strain transducers used to measure local strains in Geo-Structural Elements, ASTM Geotechnical Testing Journal. (in review)

9) Lemnitzer, A., Cox, C., Farrag, R., Turner, B. (2019): Laterally loaded shaft behavior at soil-rock impedance contrast, XVI Panamerican Conference on Soil Mechanics and geotechnical Engineering, Cancun, Mexico, November 17-20th, 2019. (Keynote paper)

10) O'Neill, M. W., & Murchison, J. M. (1983): An evaluation of p-y relationships in sands, A Report to American Petroleum Institute, PRAC 82-41-1. University of Houston

11) Reese, L. (1997). "Analysis of laterally loaded piles in weak rock". ASCE Journal of Geotechnical and Geoenvironmental Engineering, Vol. 123, No. 11

12) Slowik, V., Schlattner, E. and Klink, T. (1999): Faser-Bragg Sensoren in Bauwerken (Fiber Bragg Grating Sensors in Structures). Research Report, Leipzig University of Applied Sciences, Faculty of Civil Engineering, 1999.